frontiers | Frontiers in Energy Research

TYPE Original Research
PUBLISHED 18 November 2022
DOI 10.3389/fenrg.2022.954351

OPEN ACCESS

EDITED BY
Yanping Du,
Shanghai Jiao Tong University, China

REVIEWED BY
Elisa Marrasso,
University of Sannio, Italy
Zhu Jiang,
Southeast University, Nanjing, China

*CORRESPONDENCE
Qinmin Yang,
qmyang@zju.edu.cn

SPECIALTY SECTION
This article was submitted to Process and Energy Systems Engineering, a section of the journal Frontiers in Energy Research

RECEIVED 27 May 2022
ACCEPTED 24 October 2022
PUBLISHED 18 November 2022

CITATION
Chen X, Li C and Yang Q (2022), Adaptive finite-time fan-coil outlet wind temperature control for the ASHPAC system.
Front. Energy Res. 10:954351.
doi: 10.3389/fenrg.2022.954351

Adaptive finite-time fan-coil outlet wind temperature control for the ASHPAC system

Xiaofei Chen[1], Chao Li[1] and Qinmin Yang[1,2]*

[1]College of Control Science and Engineering, Zhejiang University, Hangzhou, Zhejiang, China, [2]Huzhou Institute of Zhejiang University, Huzhou, China

In this paper, an adaptive finite-time fan-coil outlet wind temperature control scheme is proposed for the air-source heat pump air-conditioning system. First, a correction module is introduced to compensate the first-order damp elements in the temperature sensor to capture the temperature in real-time. Then, a simple neural network is employed to approximate the unknown and nonlinear functions of the system. On this basis, an adaptive finite-time neural controller is developed, and the finite-time convergence of temperature regulation error is ensured. The stability of the studied fan-coil control is guaranteed by rigorous Lyapunov proof. Finally, two simulation examples are carried out to verify the effectiveness of the proposed control scheme.

KEYWORDS

renewable energy, ASHPAC, control, finite-time control (FTC), adaptive control

1 Introduction

Peaking carbon dioxide emissions and carbon neutrality play an important role on the national strategic level (Jia and Lin, 2021) to realize the "30· 60" goal and the "14th Five-Year Plan" for power development. It is urgent to expand the scale of renewable energy utilization and improve the energy efficiency. The ASHPAC system utilizes the solar radiating energy contained in the air as the cooling or heating source (Yu et al., 2021; Yong et al., 2021). It follows the reversible Carnot cycle when working and drives the compressor through a small amount of electricity to realize energy transfer. Compared with the general HVAC system (Magraner et al., 2010), its COP is higher. As the core component of the indoor loop of the ASHPAC system, the fan-coil performance determines the comfort of the indoor environment (Kayaci, 2020). To create a constant and comfortable indoor environment, it is of great significance to design a flexible, reliable, and stable algorithm to improve the control accuracy and response rate of the fan-coil outlet temperature.

Recently, numerous research results on the temperature control of the ASHPAC system have been reported. In Yang et al. (2007) and Grassi and Tsakalis (2000), a conventional PID scheme was proposed to deal with the temperature control problem of the ASHPAC system, but the accuracy and effectiveness would be degraded in a realistic ambience because of the varying load conditions. Thus, some modified PID schemes were proposed to improve the control performance [see (Li et al., 2013; Xu et al., 2019;

Wrat et al., 2020; Li et al., 2013; Xu et al., 2019; Wrat et al., 2020) and the references therein], where the PID parameters could be adjusted online by fuzzy reasoning, according to varying working conditions. However, these schemes are dependent on preset fuzzy rules, which require a large amount of professor knowledge, while it is difficult to establish a universal fuzzy rule base for different systems. In Han et al. (2021), a PSO fuzzy PID scheme was proposed to reduce inevitable randomness, which requires a large amount of computing resources. In Wang et al. (2021), a nonlinear MPC algorithm was proposed to regulate the temperature of outlet water of the transcritical CO_2 ASHP water heater. This scheme ensures true real-time dynamic optimization, but it requires accurate models, which are difficult to obtain. In Lissa et al. (2021), a DRL algorithm was applied to hot water tank temperature control, but it needs huge computational resources. Thus, it is still a challenging work to design an adaptive controller without prior knowledge on the requirement and accurate model for the ASHPAC system.

On the other hand, the aforementioned literature only guarantees the asymptotical convergence of the temperature regulation error, which means that the convergence time of the temperature regulation error is infinite. Different from the asymptotically stable control, the finite-time control can realize that the state tends to the equilibrium point within a finite time. With the satisfactory characteristics, such as faster convergence performance, higher control precision, and better robustness against disturbances and uncertainties, the finite-time control has been widely applied to various nonlinear systems (Yu et al., 2005; Chen et al., 2018; Li et al., 2019; Xie and Chen, 2022; Yu et al., 2005; Chen et al., 2018; Li et al., 2019; Xie and Chen, 2022). In Yu et al. (2005), a continuous finite-time control scheme was proposed for rigid robotic manipulators by constructing a new form of terminal sliding modes. Li et al. (2019) investigated the problem of adaptive finite-time tracking control for strict-feedback nonlinear continuous-time systems. In Chen et al. (2018) and Xie and Chen (2022), two different control strategies were put forward to deal with the finite-time attitude stabilization problem of the rigid spacecraft. In Emami-Naeini et al. (1994), an approximate finite-time control scheme was applied to temperature profile tracking in rapid thermal processing systems. In Chen et al. (2019), a finite-time controller was designed for the double-layer Peltier system based on a finite-time observer, such that the temperature error can be converged within a finite time. To this end, it is meaningful to design a finite-time outlet wind temperature controller for improving both the transient performance and steady performance of the ASHPAC system. However, the relevant research works on finite-time outlet wind temperature control of the ASHPAC system have not been reported.

Motivated by the aforementioned observations, an adaptive finite-time neural fan-coil outlet wind temperature control scheme is proposed for the ASHPAC system. The main contributions are summarized as follows.

Compared with the asymptotically stable control (Grassi and Tsakalis, 2000; Yang et al., 2007; Li et al., 2013; Xu et al., 2019; Wrat et al., 2020; Han et al., 2021; Lissa et al., 2021; Wang et al., 2021; Grassi and Tsakalis, 2000; Yang et al., 2007; Li et al., 2013; Xu et al., 2019; Wrat et al., 2020; Han et al., 2021; Lissa et al., 2021; Wang et al., 2021), a finite-time neural controller is systematically presented such that the temperature regulation error is ensured to converge into a small region around the origin within a finite time.

A correction module is introduced to compensate the first-order damp elements in the temperature sensor to capture the temperature in real time. Moreover, a neural network-based adaptive law is designed to compensate for the unknown and nonlinear functions of the ASHPAC system such that the model knowledge of the system is not required in prior.

The rest of this article is outlined as follows: in **Section 2**, the mathematical model is presented. The correction module of a thermistor is given in **Section 3**, and the adaptive finite-time control design and stability analysis are given in **Section 4**. In **Section 5**, the obtained results are supported by numerical simulations. Finally, the conclusion is summarized in **Section 6**.

2 System description

The ASHPAC system contains the air-source side loop, the heat pump loop, and the indoor loop (Xiao, 2010), which is shown in **Figure 1**.

As shown in **Figure 2**, the control structure of the fan-coil consists of the flow-regulating valve, the fan-coil, and the temperature sensor (Zhang et al., 2021). It is found from **Figure 2** that l and q are the spool stroke and chilled water flow at a certain opening, respectively. T_{in} is the output wind temperature of the fan-coil, T_r is the output value of the temperature sensor, and T_{in_d} is the tracking target.

Flow-regulating valves generally have four ideal flow characteristics, such as the linear characteristic, parabolic characteristic, quick opening characteristic, and equal percentage characteristic (Dutta et al., 2014).

The equal percentage flow capacity increases exponentially with the spool stroke. Equal increases in valve travel produce equal percentage changes in the existing flow coefficients. The equal percentage flow characteristic is given by Mala and Li (1999):

$$\frac{\mathrm{d}\left(\frac{q}{q_{\max}}\right)}{\mathrm{d}\left(\frac{l}{L}\right)} = K_v \frac{q}{q_{\max}}. \tag{1}$$

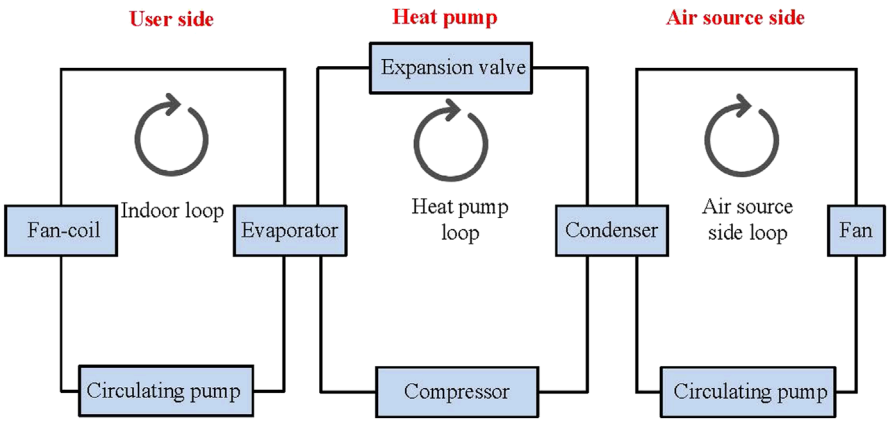

FIGURE 1
Diagram of the ASHPAC system.

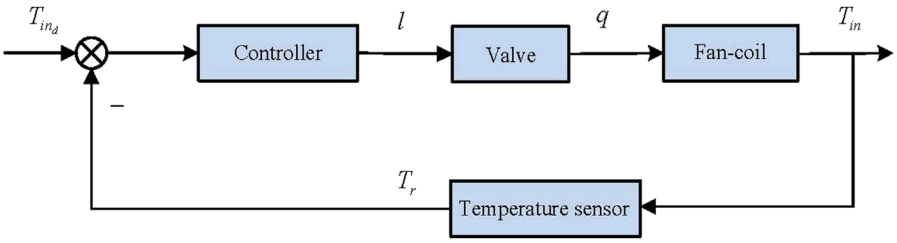

FIGURE 2
Control structure of the fan-coil.

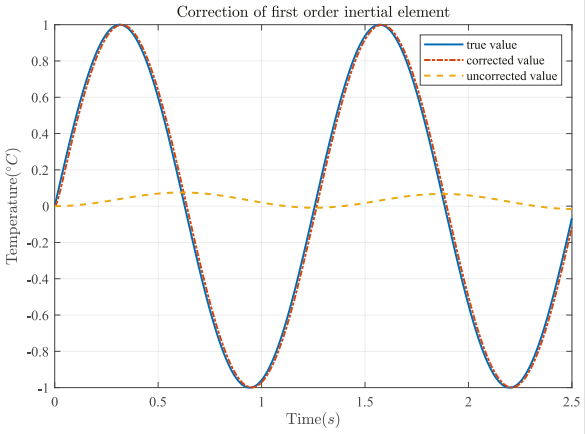

FIGURE 3
Correction of the first-order inertial element.

Using the boundary conditions

$$\begin{cases} q = q_{\min}, & l = 0 \\ q = q_{\max}, & l = L, \end{cases} \tag{2}$$

one can obtain

$$\frac{q}{q_{\max}} = \left(\frac{q_{\max}}{q_{\min}}\right)^{\left(\frac{l}{L}-1\right)}. \tag{3}$$

If $R = \frac{q_{\max}}{q_{\min}}$ is defined as the regulating ratio, then Eq. 3 can be rewritten as

$$q = q_{\min} R^{\frac{l}{L}}, \tag{4}$$

where L is the maximum spool stroke of the valve, K_v is the magnification factor, q_{max} is the maximum flow rate, and q_{min} is the minimum flow rate.

The fan-coil is the terminal device of the heat pump air-conditioning system, which is a surface heat exchanger used to reduce or increase the room temperature and create an indoor air environment suitable for human comfort.

Based on the law of energy conservation, by ignoring the heat storage effect of the fan-coil, the mathematical model can be simplified into a single-capacity first-order differential equation (Wu, 2015):

$$K_a \frac{dT_{in}}{dt} + T_{in} = -K_b q + K_c, \tag{5}$$

TABLE 1 Parameters of the system.

Parameter	Symbol	Value and unit
Constant volume-specific heat of air	C_V	$0.718kJ/(kg\cdot°C)$
Effective volume of the fan-coil	V_{fc}	$0.108m^3$
Density of air	ρ	$1.177kg/m^3$
Air supply of the fan-coil	G_{ac}	$850m^3/h$
Specific heat of air	c_1	$1.005kJ/(kg\cdot°C)$
Chilled water temperature difference	ΔT_d	$5°C$
Specific heat of chilled water	c_2	$4.2kJ/(kg\cdot°C)$
Inlet air temperature of the fan-coil	T_0	$27°C$
Total power of the fan-coil	P_0	$0.03kW$
Minimum flow rate of the valve	q_{min}	$0.008kg/s$
Regulating ratio of the valve	R	30
Maximum spool stroke of the valve	L	$12mm$
Time constant of the thermistor	T	$25s$

Computing all parameters at 27°C

TABLE 2 Objective of the tracking step signal.

Parameter	Symbol	Value
Ideal output trajectory	T_{in_d}	$24\cdot r(t)+2\cdot r(t-50)°C$
Initial output	T_{in_0}	$30°C$

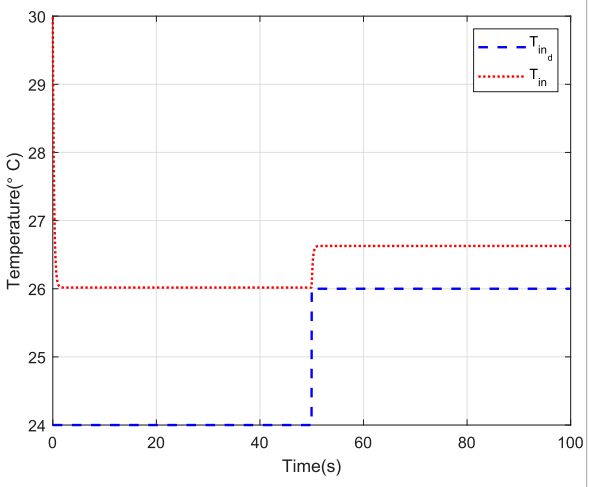

FIGURE 4
Tracking performance without NN compensation.

where $K_a=\frac{C_V V_{fc}\rho}{G_{ac}c_1}$, $K_b=\frac{\Delta T_d c_2}{G_{ac}c_1}$, and $K_c=T_0+\frac{P_0}{G_{ac}c_1}$; C_V is the constant volume-specific heat of air, V_{fc} is the volume of air circulated into the fan-coil, ρ is the density of air, G_{ac} is the air flow rate of the fan-coil, c_1 is the specific heat of air, ΔT_d is the chilled water temperature difference, c_2 is the specific heat of chilled water, T_0 is the inlet air temperature of the fan-coil, and P_0 is the total power of the fan-coil. Among these parameters, C_V, ρ, c_1, and T_0 are determined by the actual temperature, which are uncertain.

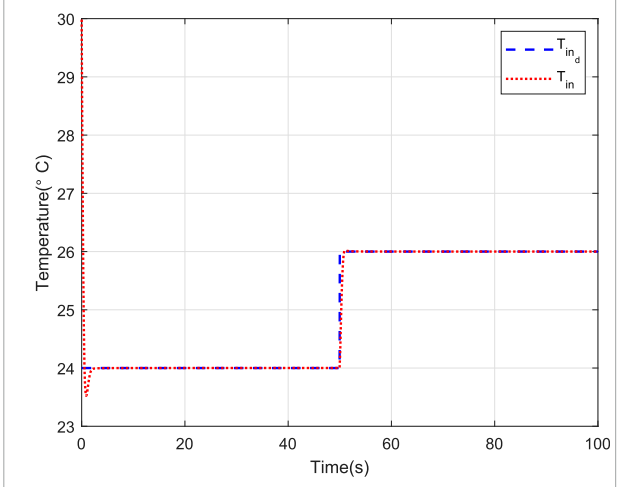

FIGURE 5
Tracking performance with NN compensation.

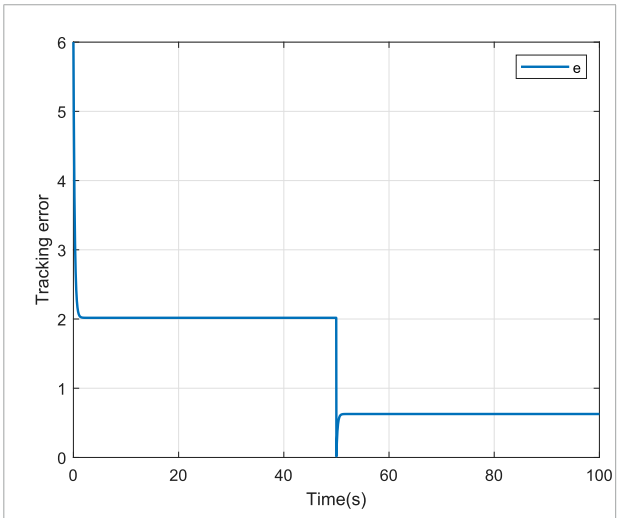

FIGURE 6
Tracking error without NN compensation.

A thermistor is often used as the temperature sensor in the closed-loop control system of air-conditioning, and the relationship between its sensed temperature T_{in} and output temperature T_r is given by

$$T\frac{dT_r}{dt}+T_r=T_{in}, \tag{6}$$

where T is the time constant of the thermistor.

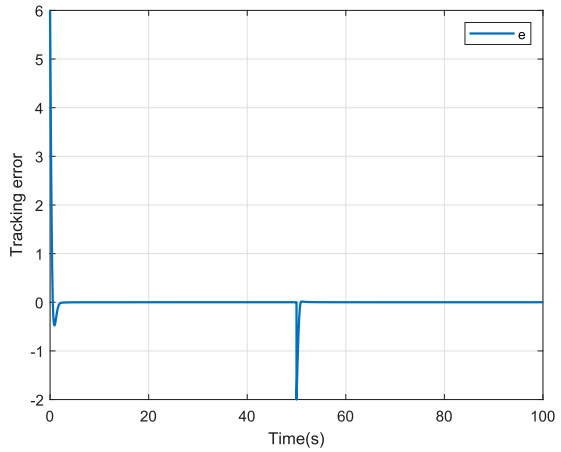

FIGURE 7
Tracking error with NN compensation.

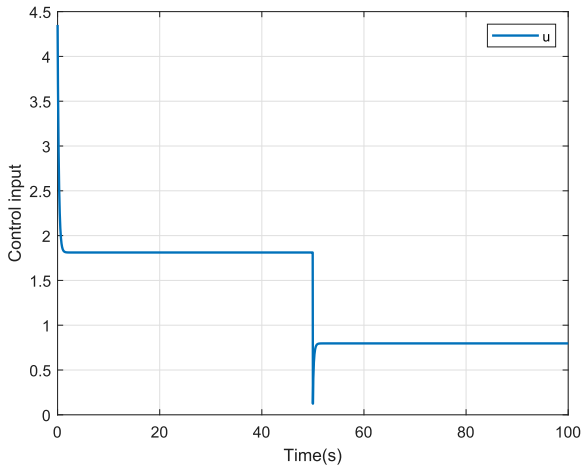

FIGURE 8
Control input without NN compensation.

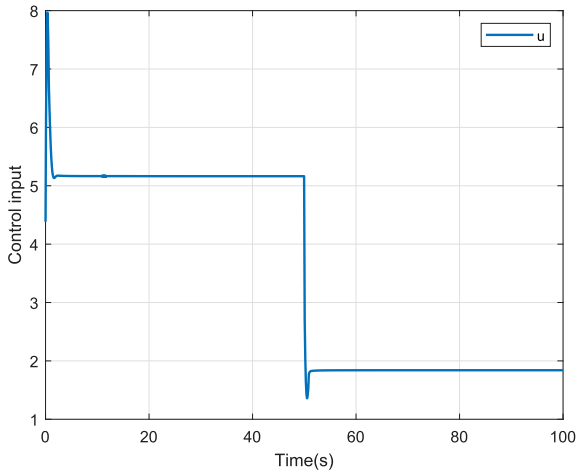

FIGURE 9
Control input with NN compensation.

TABLE 3 Objectives of the tracking squarewave and ramp signals.

Signal	Parameter	Symbol	Value
Cosine	Ideal output trajectory	T_{in_d}	$2\cos(0.3t)+20°C$
	Initial output	T_{in_0}	$30°C$

3 Correction module of the thermistor

The existence of the time constant makes the change of the thermistor thermal potential always lag behind the perceived temperature variation. Based on (6), the characteristic of the temperature sensor can be regarded as a first-order inertial element, which can be described by $G_{ts}(s)$, that is,

$$G_{ts}(s) = \frac{1}{Ts+1}. \tag{7}$$

The temperature control of the fan-coil is required to be fast and accurate; thus, the influence of T cannot be ignored. To improve the measurement accuracy of the thermistor temperature sensor, we broaden the bandwidth of the feedback element by connecting a correction element in series (Li et al., 2005), that is,

$$\begin{aligned} W(s) &= G_{ts}(s)\cdot H(s) \\ &= \frac{1}{Ts+1}\cdot\frac{Ts+1}{T's+1}, \end{aligned} \tag{8}$$

where $T' < T$, $H(s)$, and $W(s)$ are the transfer functions of the correction element and the feedback loop after correcting.

As shown in Figure 3, when the thermistor with a large time constant is used to detect the temperature directly, its output distortion is large. After adding the correction element, as long as T' is reasonably selected, the error between the sensed temperature and the output temperature can be eliminated.

4 Adaptive finite-time control

4.1 Controller design

The introduction of the correction module eliminates the lag of the thermistor, so the characteristic of the temperature sensor can be regarded as unity feedback. Based on the characteristic of the flow-regulating valve in (4), for ease of presentation, one should observe

$$q = q_{\min}u, \tag{9}$$

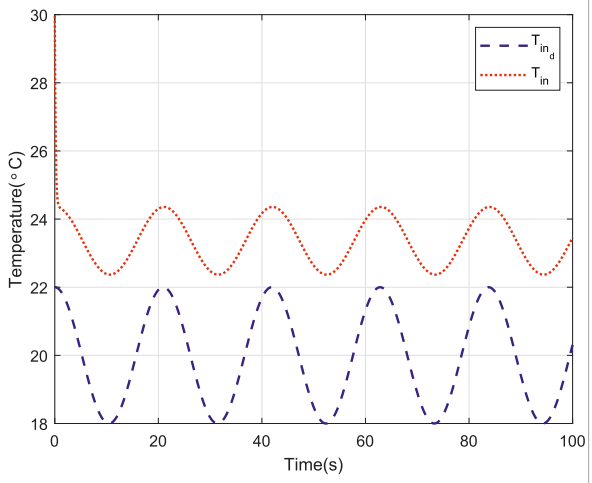

FIGURE 10
Tracking performance without NN compensation.

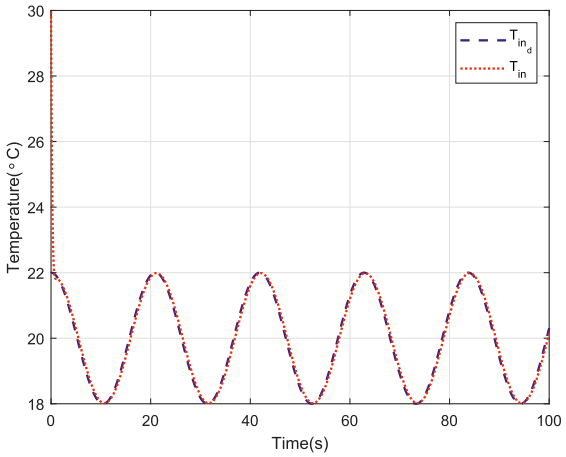

FIGURE 11
Tracking performance with NN compensation.

where $u = R^{\frac{l}{L}}$.

According to (5) and (9), one can obtain

$$\dot{T}_{in} = \frac{1}{K_a}\left(-T_{in} - K_b q_{\min} u + K_c\right), \tag{10}$$

where K_a, K_b, and K_c are uncertain in the controller design; let $\theta_1 = -\frac{1}{K_a}$, $\theta_2 = -\frac{K_b q_{\min}}{K_a}$, and $d = \frac{K_c}{K_a}$, then the fan-coil control system becomes

$$\dot{T}_{in} = \theta_1 T_{in} + \theta_2 u + d. \tag{11}$$

The tracking error e is defined as

$$e = T_{in} - T_{in_d}. \tag{12}$$

Differentiating (12) yields

$$\begin{aligned} \dot{e} &= \dot{T}_{in} - \dot{T}_{in_d} \\ &= \theta_1 T_{in} + \theta_2 u + d \\ &= \theta_2\left(\frac{\theta_1}{\theta_2} T_{in} + u + \frac{d}{\theta_2}\right) \\ &= \theta_2 (g + u), \end{aligned} \tag{13}$$

where $g = \frac{\theta_1}{\theta_2} T_{in} + \frac{d}{\theta_2}$ is the lumped uncertainty.

The lumped uncertainty g in (13) can be approximated by the neural network (NN), given by

$$g = W^T \Phi\left(T_{in}\right) + \varepsilon, \tag{14}$$

where ε is the approximation error bounded by $|\varepsilon| \le \varepsilon_N$, with ε_N being a small positive constant, and $\Phi(T_{in})$ is the NN basis function with the following sigmoid form:

$$\Phi\left(T_{in}\right) = \frac{l_1}{l_2 + \exp\left(-T_{in}/l_3\right)} + l_4. \tag{15}$$

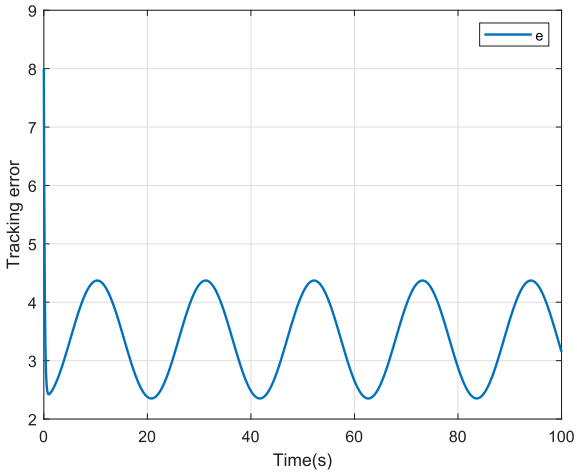

FIGURE 12
Tracking error without NN compensation.

With the NN approximation, the finite-time controller is designed as

$$u = -k_1 e - k_2 \mathrm{sig}^{\alpha}(e) - \hat{W}^T \Phi, \tag{16}$$

where $k_1 > 1/2, k_2 > 0$, $0 < \alpha < 1$, $\mathrm{sig}^{\alpha}(e) = |e|^{\alpha}\,\mathrm{sgn}(e)$, and $\mathrm{sgn}(\cdot)$ denote the sign function, and $\hat{W}$ is the estimation of W.

The adaptive update law of $\hat{W}$ is given by

$$\dot{\hat{W}} = e\Phi - \sigma \hat{W}, \tag{17}$$

where σ is a positive constant.

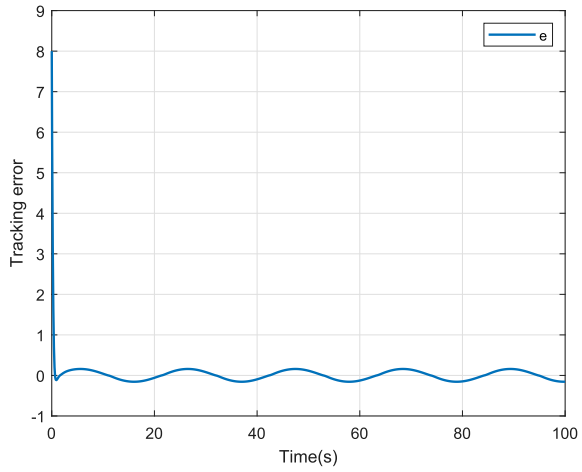

FIGURE 13
Tracking error with NN compensation.

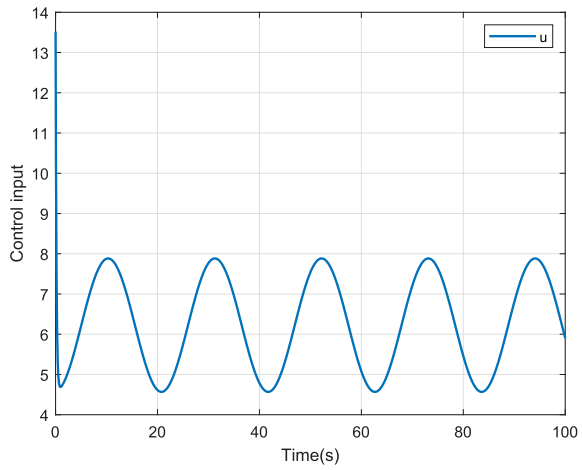

FIGURE 14
Control input without NN compensation.

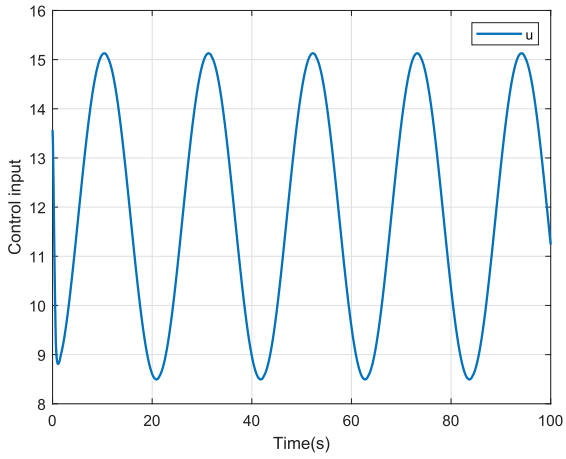

FIGURE 15
Control input with NN compensation.

4.2 Stability analysis

To analyze the finite-time stability of the fan-coil control system, several useful lemmas are provided as follows.

Lemma 1: (Xie et al., 2022): Given a system $\dot{x} = f(x)$, if there exist a continuous function $V(x)$ and scalars $\varrho_1 > 0, \varrho_2 > 0, 0 < \gamma < 1$ and $0 < \eta < \infty$ satisfying $\dot{V}(x) \leq -\varrho_1 V - \varrho_2 V^{\gamma} + \eta$, then the trajectory of the system $\dot{x} = f(x)$ is the practical finite-time stable; the residual set of the solution is calculated as $\left\{\lim_{t\to T} x \mid V(x) \leq \min\left\{\frac{\eta}{(1-\kappa)\varrho_1}, \left(\frac{\eta}{(1-\kappa)\varrho_2}\right)^{\frac{1}{\gamma}}\right\}\right\}$, where κ satisfies $0 < \kappa < 1$. The convergence time is bounded by

$$T \leq \max\left\{t_0 + \frac{1}{\kappa\varrho_1(1-\gamma)}\ln\frac{\kappa\varrho_1 V^{1-\gamma}(t_0) + \varrho_2}{\varrho_2}, t_0 + \frac{1}{\varrho_1(1-\gamma)}\ln\frac{\kappa\varrho_1 V^{1-\gamma}(t_0) + \kappa\varrho_2}{\kappa\varrho_2}\right\}.$$

Lemma 2: (Xie et al., 2022): For all positive numbers x_i, $i = 1, 2, \ldots, n$ and there exists a constant $0 < p < 1$ such that the following inequality holds:

$$\left(|x_1| + \cdots + |x_n|\right)^p < |x_1|^p + \cdots + |x_n|^p. \tag{18}$$

The following theorem is proved to show the main result of this paper.

Theorem 1: By considering the fan-coil control system (11) with the proposed finite-time controller (16) and the adaptive update law (17), it can be proved that the regulation error e can converge into a small region around the origin within a finite time.

Proof: A Lyapunov candidate function is chosen as

$$V = \frac{1}{2\theta_2}e^2 + \frac{1}{2}\tilde{W}^T\tilde{W}, \tag{19}$$

where $\tilde{W} = W - \hat{W}$.

Differentiating (19) yields

$$\dot{V} = \frac{1}{\theta_2}e\dot{e} - \tilde{W}^T\dot{\hat{W}}. \tag{20}$$

Substituting (13) and (14) into (20) gives

$$\dot{V} = e\left(W^T\Phi + \varepsilon + u\right) - \tilde{W}^T\dot{\hat{W}}. \tag{21}$$

Substituting (16) into (21) yields

$$\begin{aligned}\dot{V} &= e\left(W^T\Phi + \varepsilon - k_1 e - k_2 \mathrm{sig}^{\alpha}(e) - \hat{W}^T\Phi\right) \\ &\quad - \tilde{W}^T\dot{\hat{W}} \\ &= e\tilde{W}^T\Phi + e\varepsilon - k_1 e^2 - k_2|e|^{1+\alpha} - \tilde{W}^T\dot{\hat{W}} \\ &= \tilde{W}^T\left(e\Phi - \dot{\hat{W}}\right) + e\varepsilon - k_1 e^2 - k_2|e|^{1+\alpha}. \end{aligned} \tag{22}$$

Substituting (17) into (22) yields

$$\dot{V} = \sigma\tilde{W}^T\hat{W} + e\varepsilon - k_1 e^2 - k_2|e|^{1+\alpha}. \tag{23}$$

According to Young's inequality, one can obtain

$$\sigma\tilde{W}^T\hat{W} = \sigma\tilde{W}^T\left(W - \hat{W}\right) \le -\frac{3}{4}\sigma\|\tilde{W}\|^2 + \sigma\|W\|^2, \tag{24}$$

$$\left(\frac{\sigma\|\tilde{W}\|^2}{2}\right)^{\frac{1+\alpha}{2}} - \frac{\sigma\|\tilde{W}\|^2}{2} \le \frac{1}{4}, \tag{25}$$

and

$$e\varepsilon \le \frac{e^2}{2} + \frac{\varepsilon_N^2}{2}. \tag{26}$$

Substituting (24)–(26) into (23) gives

$$\begin{aligned}\dot{V} &\le -\left(k_1 - \frac{1}{2}\right)e^2 - k_2|e|^{1+\alpha} - \frac{\sigma}{4}\|\tilde{W}\|^2 - \frac{\sigma}{2}\|\tilde{W}\|^2 \\ &\quad + \sigma\|W\|^2 + \frac{\varepsilon_N^2}{2} \\ &\le -\bar{k}_1 e^2 - k_2|e|^{1+\alpha} - \frac{\sigma}{4}\|\tilde{W}\|^2 - \left(\frac{\sigma\|\tilde{W}\|^2}{2}\right)^{\frac{1+\alpha}{2}} \\ &\quad + \frac{1}{4} + \sigma\|W\|^2 + \frac{\varepsilon_N^2}{2}, \end{aligned} \tag{27}$$

where $\bar{k}_1 = k_1 - \frac{1}{2}$.

According to **Lemma 2**, one can obtain

$$\dot{V} \le -\mu_1 V - \mu_2 V^{\frac{1+\alpha}{2}} + \eta, \tag{28}$$

where $\mu_1 = \min\{2\theta_2\bar{k}_1, \frac{\sigma}{4}\}$, $\mu_2 = \min\{(2\theta_2)^{\frac{1+\alpha}{2}}, \sigma^{\frac{1+\alpha}{2}}\}$, and $\eta = \frac{1}{4} + \sigma\|W\|^2 + \frac{\varepsilon_N^2}{2}$.

According to **Lemma 1**, the fan-coil control system (11) is practically finite-time stable, and the regulation error e can converge into the following region Δ, that is,

$$\Delta = \left\{\lim_{t\to t_r} e \mid V \le \min\left\{\frac{\eta}{(1-\kappa)\mu_1}, \left(\frac{\eta}{(1-\kappa)\mu_2}\right)^{\frac{2}{1+\alpha}}\right\}\right\}, \tag{29}$$

where

$$\begin{aligned} t_r \le \max\Bigg\{&\frac{1}{\kappa\mu_1(1-\alpha)}\ln\frac{\kappa\mu_1 V^{1-\alpha}(0) + \mu_2}{\mu_2}, \\ &\frac{1}{\mu_1(1-\alpha)}\ln\frac{\kappa\mu_1 V^{1-\alpha}(0) + \kappa\mu_2}{\kappa\mu_2}\Bigg\} \end{aligned} \tag{30}$$

and $0 < \kappa < 1$.

5 Simulation results

We choose the fan-coil "SF05RC" produced by PHNIX and the electric small flow-regulating valve produced by VTON as objects and compute the parameters of the system in Table 1, and the units of measurements of these terms are provided.

The models of the flow-regulating valve, the fan-coil, and the temperature sensor are given as

$$q = 0.008 \cdot 30^{\frac{l}{12}}, \tag{31}$$

$$0.3275\frac{\mathrm{d}T_{in}}{\mathrm{d}t} + T_{in} = -75.19q + 27.107. \tag{32}$$

Based on this system model, the proposed adaptive finite-time controller is then utilized. Also, the unknown parameters are initialized with $K_a = 0.3275s$, $K_b = 75.1900\,(°C\cdot s)/kg$, and $K_c = 27.1070°C$. The parameters of the finite-time controller (16) and adaptive update law (17) are chosen as $k_1 = 2, k_2 = 2, \alpha = \frac{5}{7}$ and $\sigma = 0.1$. The parameters of the sigmoid function (15) are set as $l_1 = 12, l_2 = 10, l_3 = 6$, and $l_4 = 2$.

5.1 Simulation with the step signal

The tracking objective is chosen as Table 2 for controlling the step signal, where $r(t)$ is the step signal.

To verify the effectiveness of the proposed scheme, two comparative cases, that is, without and with the NN compensation are provided. For fair comparison, the parameters of the two schemes are selected the same. The corresponding simulation results are depicted in Figures 4–9. Figure 4 shows the tracking performance without NN compensation. From Figure 4, it can be seen that the output wind temperature of the fan-coil cannot reach the first target (24°C) and the second target (26°C) in a short time. Figure 5 depicts the tracking performance with NN compensation. It can be found from Figure 5 that the tracking performance is superior. Compared with Figures 4, 5, we can conclude that the finite-time controller can realize fast and accurate temperature regulation with the help of the NN compensation. The temperature tracking error e without and with NN compensation are shown in Figures 6, 7, respectively. From Figure 6, it can be seen that the temperature tracking error e is large. From Figure 7, we can see that when the temperature changes rapidly, the temperature tracking error e becomes lager, but the temperature tracking error e is small overall. In addition, the control input u without and with NN compensation are depicted in Figures 8, 9, respectively. From Figures 8, 9, it can be obtained that the larger control input is required with NN compensation.

5.2 Simulation with the cosine signal

Furthermore, we also simulate the proposed adaptive control algorithm with the cosine signal, and the objectives are chosen as **Table 3**.

The results of the tracking cosine signal are shown in **Figures 10–15**. **Figure 10** shows the tracking performance without NN compensation. From **Figure 10**, it can be seen that the output wind temperature of the fan-coil cannot reach the target temperature. **Figure 11** depicts the tracking performance with NN compensation. It can be found from **Figure 11** that the tracking performance is superior with a fast response. The temperature tracking error e without and with NN compensation are shown in **Figures 12**, **13**, respectively. From **Figures 12**, **13**, we can again obtain that the temperature tracking error e is smaller with the aid of NN compensation. Moreover, the control input u without and with NN compensation are depicted in **Figures 14**, **15**, respectively. From **Figures 14**, **15**, we can again obtain that the larger control input is required with NN compensation.

From **Figures 4–15**, it can be concluded that the proposed control scheme can achieve the satisfactory tracking performance (e.g., fast convergence speed and accurate tracking error) with the help of NN compensation.

6 Conclusion

In this paper, an adaptive finite-time fan-coil outlet wind temperature control scheme has been developed for the air-source heat pump air-conditioning system. A correction module is introduced to compensate for the first-order damp elements in the temperature sensor to capture the temperature in real time. On this basis, an adaptive finite-time neural controller is developed. Different from the asymptotically stable control, the proposed finite-time temperature control can ensure that the temperature regulation error be converged into a small region around the origin within a finite time, which further improves the tracking performance of the ASHPAC system. Finally, two simulation examples have been carried out to demonstrate the effectiveness of the proposed scheme.

Data availability statement

The datasets generated and analysed during the current study are not publicly available as the data also forms part of an ongoing study, but are available from the corresponding author on reasonable request.

Author contributions

CL and QY contributed to the conceptionand design of the study. XC organized the database and performed the statistical analysis. All authors contributed in drafting the manuscript and revision. They approved the submitted version.

Conflict of interest

The authors declare that the research was conducted in the absence of any commercial or financial relationships that could be construed as a potential conflict of interest.

Publisher's note

All claims expressed in this article are solely those of the authors and do not necessarily represent those of their affiliated organizations, or those of the publisher, the editors, and the reviewers. Any product that may be evaluated in this article, or claim that may be made by its manufacturer, is not guaranteed or endorsed by the publisher.

References

Chen, C., Ding, S., and Li, S. (2019). Finite-time control for double-layer Peltier system based on finite-time observer. *Adv. Mech. Eng.* 11 (3), 168781401983685–10. doi:10.1177/1687814019836852

Chen, Q., Xie, S., Sun, M., and He, X. (2018). Adaptive nonsingular fixed-time attitude stabilization of uncertain spacecraft. *IEEE Trans. Aerosp. Electron. Syst.* 54 (6), 2937–2950. doi:10.1109/taes.2018.2832998

Dutta, S., Sarkar, A., Samanta, K., Das, R., and Ghosh, A. (2014). "Supervision of control valve characteristics using PLC and creation of HMI by SCADA," in 2014 First International Conference on Automation, Control, Energy and Systems (ACES), 1–5.

Emami-Naeini, A., Kabuli, M., and Kosut, R. (1994). "Finite-time tracking with actuator saturation: Application to RTP temperature trajectory following," in 33rd IEEE Conference on Decision and Control, 73–78.

Grassi, E., and Tsakalis, K. (2000). PID controller tuning by frequency loop-shaping: Application to diffusion furnace temperature control. *IEEE Trans. Control Syst. Technol.* 8 (5), 842–847. doi:10.1109/87.865857

Han, Q., Yang, Y., Yu, J., Gu, H., Ren, X., and Gao, L. (2021). "Design of heat pump temperature control system based on particle swarm optimization fuzzy PID," in 2021 36th Youth Academic Annual Conference of Chinese Association of Automation (YAC), 442–446.

Jia, Z., and Lin, B. (2021). How to achieve the first step of the carbon-neutrality 2060 target in China: The coal substitution perspective. *Energy* 233, 121179. doi:10.1016/j.energy.2021.121179

Kayaci, N. (2020). Energy and exergy analysis and thermo-economic optimization of the ground source heat pump integrated with radiant wall panel and fan-coil unit with floor heating or radiator. *Renew. Energy* 160, 333–349. doi:10.1016/j.renene.2020.06.150

Li, H., Zhao, S., He, W., and Lu, R. (2019). Adaptive finite-time tracking control of full state constrained nonlinear systems with dead-zone. *Automatica* 100, 99–107. doi:10.1016/j.automatica.2018.10.030

Li, Q., Li, G., and Zhang, T. (2005). The thermo-couple dynamic characteristic correction. *Electron. Meas. Technol.* 3 (18), 32–33.

Li, Y., Cai, C., Lee, K., and Teng, F. (2013). A novel cascade temperature control system for a high-speed heat-airflow wind tunnel. *Ieee. ASME. Trans. Mechatron.* 18 (4), 1310–1319. doi:10.1109/tmech.2013.2262077

Lissa, P., Deane, C., Schukat, M., Seri, F., Keane, M., and Barrett, E. (2021). Deep reinforcement learning for home energy management system control. *Energy AI* 3, 100043. doi:10.1016/j.egyai.2020.100043

Magraner, T., Montero, A., Quilis, S., and Urchueguía, J. F. (2010). Comparison between design and actual energy performance of a HVAC-ground coupled heat pump system in cooling and heating operation. *Energy Build.* 42 (9), 1394–1401. doi:10.1016/j.enbuild.2010.03.008

Mala, G., and Li, D. (1999). Flow characteristics of water in microtubes. *Int. J. heat fluid flow* 20 (2), 142–148. doi:10.1016/s0142-727x(98)10043-7

Wang, W., Zhao, Z., Zhou, Q., Qiao, Y., and Cao, F. (2021). Model predictive control for the operation of a transcritical CO2 air source heat pump water heater. *Appl. Energy* 300, 117339. doi:10.1016/j.apenergy.2021.117339

Wrat, G., Bhola, M., Ranjan, P., Mishra, S. K., and Das, J. (2020). Energy saving and Fuzzy-PID position control of electro-hydraulic system by leakage compensation through proportional flow control valve. *ISA Trans.* 101, 269–280. doi:10.1016/j.isatra.2020.01.003

Wu, D. (2015). *Modeling and simulation of central air-conditioning automatic control system*. Hohhot, China: Inner Mongolia University.

Xiao, X. (2010). *Study of energy-saving control system in ground-source heat pump central air-conditioner*. Changsha, China: Hunan Normal University.

Xie, S., and Chen, Q. (2022). Adaptive nonsingular predefined-time control for attitude stabilization of rigid spacecrafts. *IEEE Trans. Circuits Syst. Ii.* 69 (1), 189–193. doi:10.1109/tcsii.2021.3078708

Xie, S., Chen, Q., and He, X. (2022). Predefined-time approximation-free attitude constraint control of rigid spacecraft. *IEEE Trans. Aerosp. Electron. Syst.*, 1–11. doi:10.1109/TAES.2022.3183550

Xu, Y., Jia, M., and Chen, S. (2019). "Research on electric vehicle heat pump air conditioning control system based on fuzzy PID algorithm," in 2019 Chinese Automation Congress (CAC), 1155–1159.

Yang, Z., Pedersen, G. K. M., Larsen, L. F. S., and Thybo, H. (2007). "Modeling and control of indoor climate using a heat pump based floor heating system," in IECON 2007 - 33rd Annual Conference of the IEEE Industrial Electronics Society, 2985–2990.

Yong, H. E., Chung, Y., Min, S. P., Hong, S. B., and Min, S. K. (2021). Deep learning-based prediction method on performance change of air source heat pump system under frosting conditions. *Energy* 228, 120542. doi:10.1016/j.energy.2021.120542

Yu, M., Li, S., Zhang, X., and Zhao, Y. (2021). Techno-economic analysis of air source heat pump combined with latent thermal energy storage applied for space heating in China. *Appl. Therm. Eng.* 185, 116434. doi:10.1016/j.applthermaleng.2020.116434

Yu, S., Yu, X., Shirinzadeh, B., and Man, Z. (2005). Continuous finite-time control for robotic manipulators with terminal sliding mode. *Automatica* 41 (11), 1957–1964. doi:10.1016/j.automatica.2005.07.001

Zhang, T., Li, Y., Yang, Q., Meng, W., and Jiang, H. (2021). Adaptive fan-coil outlet wind temperature control with correction module of thermistor for the ASHPAC system. *in 2021 China Automation Congress (CAC)*, 7955–7960.

Nomenclature

Abbreviations

ASHPAC air-source heat pump air-conditioning
HVAC heating ventilation air-conditioning
COP coefficient of performance
PSO particle swarm optimization
MPC model predictive control
ASHP air-source heat pump
DRL deep reinforcement learning
PID proportional integral derivative.